Waves Random Media **9** (1999) 27–36. Printed in the UK PII: S0959-7174(99)90395-6

Effect of absorption on surface speckles in random media

S Sangu†, T Okamoto‡, J Uozumi† and T Asakura§

† Research Institute for Electronic Science, Hokkaido University, Sapporo, Hokkaido 060-0812, Japan

‡ Department of Control Engineering and Science, Kyushu Institute of Technology, Iizuka, Fukuoka 820-8502, Japan

§ Faculty of Engineering, Hokkai-Gakuen University, Sapporo, Hokkaido 064-0926, Japan

Received 5 January 1998, in final form 14 July 1998

Abstract. We investigate the intensity fluctuations of light backscattered from absorbing random media. A numerical simulation which takes into account the interference among different scattering paths reveals that the contrast of speckle patterns appearing at the surface of the medium decreases with an increase of absorption in weak absorption regime, but increases for strong absorption. It is shown from a simple theoretical model that such a contrast variation is caused by changes in the power of diffusive-scattering waves and in the amplitude distribution of single and low-order scattering waves.

1. Introduction

Optical coherent phenomena in multiple-scattering media have been discussed in many articles since they are connected with such applications as biomedical imaging, optical characterization of random media, and tools for the interpretation of complex systems. Most of these studies are based on a photon random-walk model which gives a diffusive character to the light inside the scattering medium. In some cases, however, we cannot ignore the interference phenomena in the multiply-scattered light, such as long-range intensity correlations over a few speckle spots [1–3], non-Rayleigh statistics of intensity fluctuations [4–7] and coherent backscattering effects [8–10].

In this paper, we discuss the effect of light absorption of random media on the statistical properties of speckles arising at the surface of the medium. The contribution of the absorption to the interference phenomena which appear in a multiple-scattering regime has been investigated from different aspects: for example, the correlation properties of light in spatial and spectral domains [11, 12] and non-Rayleigh statistics of intensity fluctuations in absorbing random media [6]. Those studies mainly discussed the properties of the highly scattered light. We pay special attention to the intensity properties of backscattered light which include both the low- and higher-order scattering components at the front surface of the medium.

In strong absorbing media, the amplitude of multiply-scattered waves with long optical paths becomes smaller than in non-absorbing media. However, the first-order statistical properties of intensity fluctuations caused by these waves are not modified, except for a decrease in the average intensity, because the central-limit theorem still holds for the scattering amplitudes forming a speckle field at the sample surface. On the other hand, the low-order scattering may give a more complex effect on the statistical properties of backscattered light. We examine two factors which determine the speckle contrast defined by the average intensity

0959-7174/99/010027+10$19.50

ratio of the low-order scattering components to the higher-order scattering components, and the amplitude modulation caused by the light absorption. The former factor is governed by the sample thickness and the scattering anisotropy.

In section 2, we explain numerical simulations based on the wave transport. Our simulations are different from the photon random-walk model, and include the dependence of the absorption effect on the particle–particle distance. Some simulation results on a variation of the speckle contrast are presented in section 3. In section 4, we propose a simple theoretical model and discuss the physical meaning of the contrast variation. Conclusions are given in the last section.

2. Simulation method

We use a numerical simulation which was proposed by Edrei *et al* [13]. In this simulation, the scattering amplitude was calculated by assigning a $2D \times 2D$ S-matrix at each site on a lattice, with D being the sample dimensionality. The S-matrix includes both the energy distribution in different directions due to scattering and the phase distribution from 0 to 2π due to scattering and propagation in free space. In order to introduce the absorption effect, we divide the S-matrix into the two parts of scattering and free propagation. We restrict our discussion to the two-dimensional case for a better understanding of the physical meaning of interference phenomena.

A scattering event is described as follows:

$$\boldsymbol{A}^{(l,m)}(n+1) = \boldsymbol{F}^{(l,m)}\boldsymbol{S}^{(l,m)}\boldsymbol{A}^{(l,m)}(n) \qquad \begin{pmatrix} 1 \leqslant l \leqslant L \\ 1 \leqslant m \leqslant W \end{pmatrix} \tag{1}$$

where $\boldsymbol{A}^{(l,m)}(n)$ denotes a vector of scattering amplitudes on the scatterer (l, m) at the nth time step, $\boldsymbol{S}^{(l,m)}$ is an S-matrix which relates input amplitudes to output amplitudes, and $\boldsymbol{F}^{(l,m)}$ is a matrix which has only diagonal elements for representing the free propagation of light between scattering particles (see figure 1). L and W represent the numbers of scatterer blocks in the longitudinal direction and the transverse direction, respectively. The S-matrix elements obey unitarity for energy conservation and symmetry for isotropic scatterers. They are given by

$$\boldsymbol{S}_{ij}^{(l,m)} = \begin{cases} |r|\mathrm{e}^{\mathrm{i}\phi_r} & i = j \\ |t|\mathrm{e}^{\mathrm{i}\phi_t} & i = 2D - (j-1) \\ |v|\mathrm{e}^{\mathrm{i}\phi_v} & \text{otherwise} \end{cases} \tag{2}$$

where the indices r, t and v denote the reflection, transmission and vertically scattering components, respectively. The indices i and j represent the row and the column numbers of the

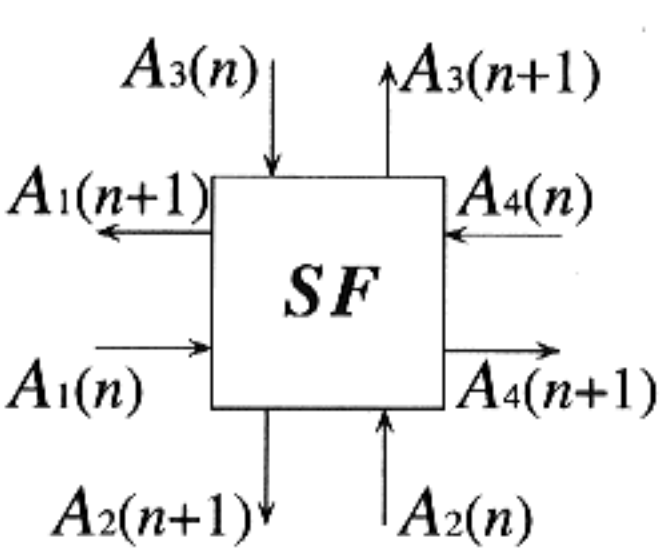

Figure 1. Schematic representation of a two-dimensional model of a scatterer. The input waves, $A_i^{(l,m)}(n)$, are divided into four orthogonal directions with the amplitude $A_i^{(l,m)}(n+1)$ by the matrices $S^{(l,m)}$ and $F^{(l,m)}$, where $i = 1, 2, 3, 4$.

S-matrix and correspond to the incident and the output directions at the scatterer, respectively. The matrix $\boldsymbol{F}^{(l,m)}$ is written as

$$\boldsymbol{F}_{ij}^{(l,m)} = \begin{cases} \exp\left(\mathrm{i}ks_i - \dfrac{s_i}{2l_a}\right) & i = j \\ 0 & \text{otherwise.} \end{cases} \tag{3}$$

The matrix $\boldsymbol{F}^{(l,m)}$ has identical elements with neighbouring sites, i.e. $\boldsymbol{F}_{11}^{(l,m)} = \boldsymbol{F}_{44}^{(l,m-1)}$ and $\boldsymbol{F}_{22}^{(l,m)} = \boldsymbol{F}_{33}^{(l-1,m)}$, which reproduce a time-reversal symmetry of the scattered light. The length s_i stands for a particle–particle distance, and l_a denotes an absorption length obeying the Lambert–Beer law. Therefore, the latter term in the exponential of equation (3) represents the amplitude loss caused by absorption during propagation in free space.

In order to incorporate the absorption effect into the existing matrix method, we need to know the path length distribution between scattering events. With the assumption of a homogeneous random medium, the distance between two scattering particles has the probability density distribution of exponential decay:

$$p(s_i) = \frac{1}{l}\exp\left(-\frac{s_i}{l}\right) \tag{4}$$

where l is the mean free path. For simplicity, all length scales are normalized by l and, then, the parameters which should be taken into consideration are kl which is called a Ioffe–Regel product, the normalized absorption coefficient $\gamma \equiv (l_a/l)^{-1}$, and the S-matrix elements relating to the scattering anisotropy. We set $kl = 500$ in numerical simulations. This condition means that the average distance between the scatterers is sufficiently larger than the wavelength of the incident light. Therefore, the phase change due to the free propagation is distributed almost uniformly between 0 and 2π.

Here we state comparisons between the simulations and the real experimental case. The purpose of this simulation is to reproduce interference effects which are induced by the optical waves propagating through the same parts of optical paths in a medium, such as a non-Rayleigh distribution of intensity fluctuations [4] and long-range correlation properties [14, 15]. The restriction of the orthogonal scattering directions in simulations readily gives a large number of paths which contribute to such interference effects. In the experimental case, these paths would also occur in a strong scattering regime, but would be much fewer than those generated by the simulations. On the other hand, we do not consider any parameters which denote sample structures such as, for example, size, shape and spatial distribution of particles. From the analogies of rough surface scattering, these parameters may contribute to an angular dependence of the single or the low-order scattered light [16] even for a speckle pattern which is observed at the surface of the medium. In our simulations, such a contribution of the particle geometry is not taken into consideration, except for giving the scattering anisotropy to the S-matrix. Therefore, we ignore these parameters by making the assumption that particles are point-like scatterers. The angular dependence of the scattered light vanishes because of this assumption and in accordance with the spatial distribution of scatterers, being dispersed randomly and isolated from each other at a large distance in comparison with the wavelength of the incident light.

Supplying a unit amplitude which indicates an input plane wave with a direction normal to the sample surface, we continue the calculations until the total transmitted intensity reaches a steady state. The reflective boundary conditions are applied on both sides, $m = 1$ and $W(= 128)$, and the S-matrices are multiplied by the matrices $\boldsymbol{F}^{(1,m)}$ at the input plane of $l = 1$ for the free propagation before the first scattering events. In what follows, we analyse the statistics of intensity fluctuations in the output field across the sample surface from which the input plane wave is fed continuously.

3. Simulation results

In figure 2, we show probability density distributions of the normalized intensity with absorption coefficients of $\gamma = 0, 0.05$ and 0.3, which are typical values for the non-absorption regime, the weak absorption regime, and the strong absorption regime, respectively. These regimes are distinguished from each other by their own properties of intensity fluctuations. For the weak absorption of $\gamma = 0.05$, the probability observed for $I/\langle I\rangle > 2.5$ is lower than that for non-absorption, and a deviation from the Rayleigh statistics is large. In the strong absorption regime of $\gamma = 0.3$, however, the density distribution of the intensity fluctuations approaches that of the Rayleigh statistics.

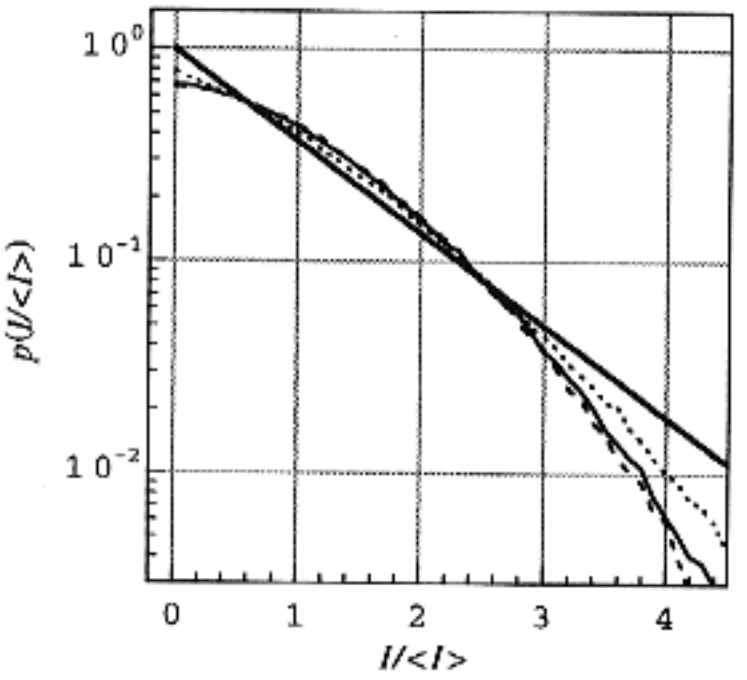

Figure 2. Probability density function of the normalized intensity. The solid, dashed, and dotted curves are for absorption coefficients of $\gamma = 0$, 0.05 and 0.3, respectively. The bold line represents a negative exponential decay which is characteristic of the Rayleigh statistics.

We consider two mechanisms which are responsible for the variation of the intensity fluctuations in absorbing media. The first mechanism is based on the fact that the weak absorption makes the contribution of the higher-order scattering components smaller than in non-absorbing media. As a result, the low-order scattering components, which take approximately a constant amplitude but are not in phase, become more dominant at any point in the output field. We can observe this effect by comparing the density curves for $\gamma = 0$ and 0.05 in figure 2, and by recognizing that the intensity fluctuations are suppressed for $\gamma = 0.05$. Comparing the curves for $\gamma = 0.05$ and 0.3, however, we observe an increase in the intensity fluctuations for the stronger absorption. This is explained by the second mechanism, being caused by the strong amplitude decay due to the absorption. The strong intensity fluctuations observed in this absorption regime arise from the fluctuations of the amplitude itself for the low-order scattering components.

We discuss a variation of the speckle contrast in order to evaluate the contribution from such mechanisms of absorption to the intensity fluctuations. The speckle contrast is defined as

$$C = \frac{\sigma}{\langle I\rangle} \tag{5}$$

where σ denotes a standard deviation of the scattering intensity. The contrast becomes unity when the intensity fluctuations obey Rayleigh statistics. Figure 3 shows the speckle contrast against the absorption coefficients for $L = 5$ and 15. It clearly shows the behaviour mentioned above: as the absorption becomes stronger, the speckle contrast first decreases and then increases constantly. Since the low-order scattering components are more dominant for $L = 5$ than for $L = 15$, the contrast for $L = 5$ is smaller than that for $L = 15$ in the case of

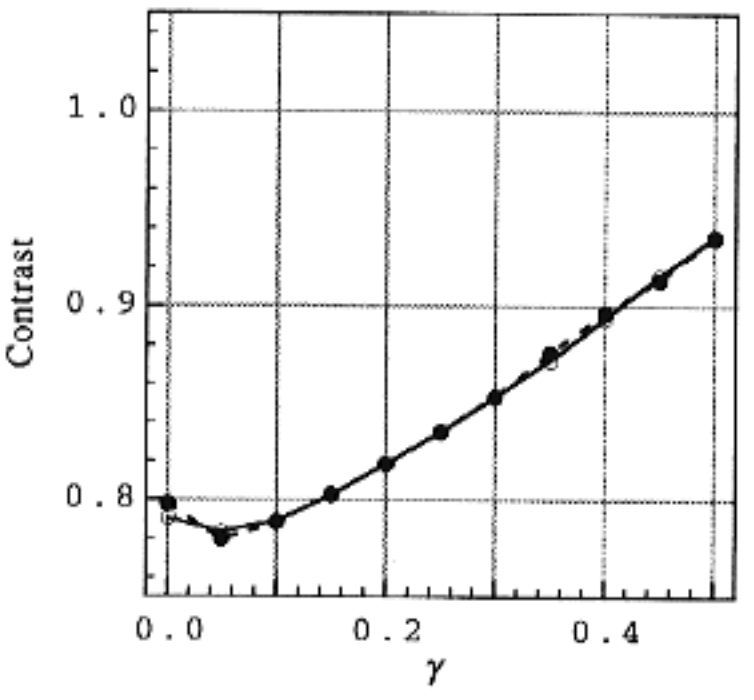

Figure 3. Speckle contrast versus the absorption coefficient γ for an isotropic scattering of $g = 0$. The open circles (○) and filled circles (●) denote the data for the sample thicknesses of $L = 5$ and 15, respectively.

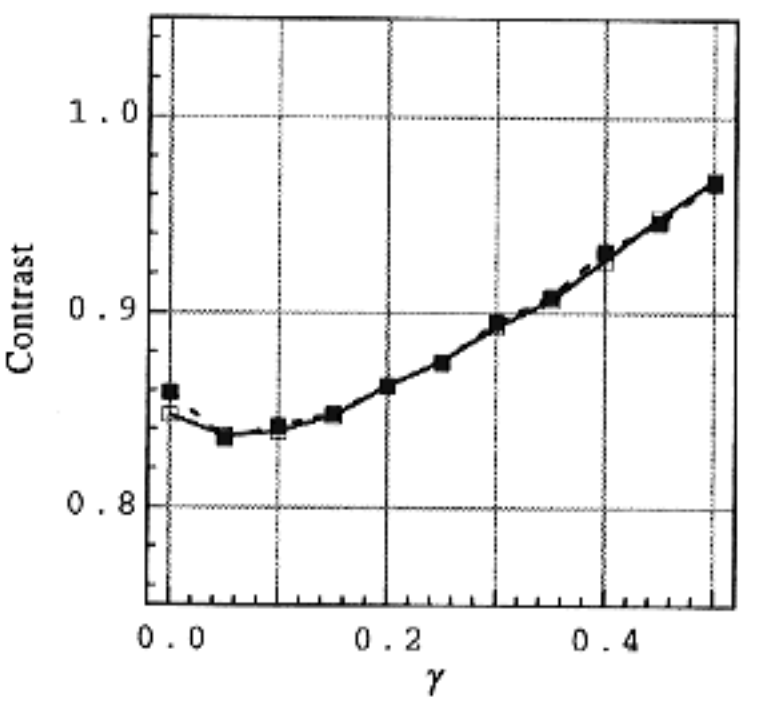

Figure 4. Speckle contrast versus the absorption coefficient γ for an asymmetry factor of $g = 0.33$. The open squares (□) and filled squares (■) denote the data for the sample thicknesses of $L = 5$ and 15, respectively.

non-absorption $\gamma = 0$. We see a variation of the contrast with the sample thickness only in the weak absorption regime of $\gamma < 0.1$, and the contrast is almost the same for both $L = 5$ and 15 in the strong absorption regime. This fact indicates that, in the weak absorption regime, the high-order scattering with long optical paths beyond the sample thickness $L = 5$ becomes small for $L = 15$, with an increase in the absorption, and that it no longer contributes to the intensity statistics in the strong absorption regime.

Next, we change the scattering anisotropy to control the average intensity ratio of the low-order scattering components to the higher-order components. Figure 4 shows a variation of the contrast with the asymmetry factor $g = \langle \cos\theta \rangle \approx 0.33$, θ being the scattering angle for a single scatterer with respect to the direction of the incident light. The properties of the intensity fluctuations are close to those of the Rayleigh statistics for $g \approx 0.33$ because of a decrease in the low-order scattering components. The variation of the contrast with the absorption is almost the same as in the case of $g = 0$.

At this stage, we cannot estimate the average intensity ratio of the low-order scattering components to the higher-order components. In the next section, we will evaluate this ratio from a simple theoretical model, and discuss the results.

4. Theoretical investigation

We consider a simple model in which the scattering amplitude is separable into two parts of low-order scattering and diffusive-scattering components. The low-order scattering component has approximately a constant amplitude in the non-absorbing case and causes a deviation of the intensity fluctuations from Rayleigh statistics, while the diffusive-scattering component shows Gaussian statistics for the complex amplitude. In figure 5, the phasors including both the components are illustrated in the complex plane. The scattering amplitude is given by

$$A = |A_c| e^{i\phi_c} + \sum_{i=1}^{N} |A_i| e^{i\phi_i} \tag{6}$$

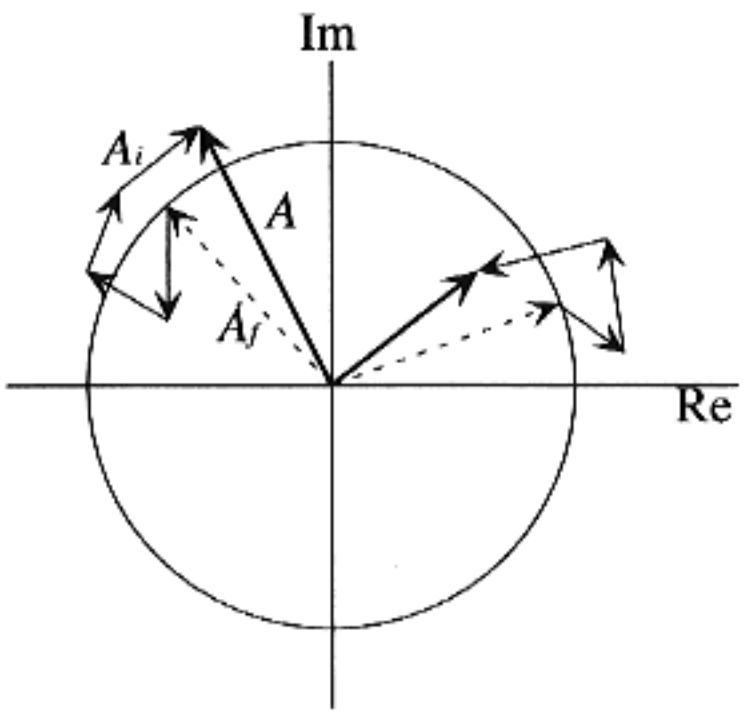

Figure 5. Phasors of the scattering amplitudes in the complex plane. The circle indicates the magnitude of a nearly constant amplitude of the low-order scattering components.

where the indices c and i denote the low-order scattering part with a nearly constant amplitude and a partial wave of the diffusive-scattering part, respectively, and the exponential terms are the phase variations due to both the free propagation and the scattering events. The average intensity is readily derived as

$$\langle I \rangle \simeq \langle |A_c|^2 \rangle + \left\langle \sum_{i=1}^{N} \sum_{j=1}^{N} |A_i||A_j| \exp[\mathrm{i}(\phi_i - \phi_j)] \right\rangle$$

$$\simeq \langle |A_c|^2 \rangle + \sum_{i=j}^{N} \langle |A_i|^2 \rangle \tag{7}$$

and the second-order momentum is also derived as

$$\langle I^2 \rangle \simeq \langle |A_c|^4 \rangle + 4\langle |A_c|^2 \rangle \sum_{i=j}^{N} \langle |A_i|^2 \rangle + 2\left(\sum_{i=j}^{N} \langle |A_i|^2 \rangle \right)^2 \tag{8}$$

where no correlation has been assumed to exist between the partial waves in the diffusive-scattering part and, thus, the second-order and fourth-order correlation terms of scattering amplitudes survive only for $\phi_i = \phi_j$ in equation (7) and for $\phi_i = \phi_j$, $\phi_k = \phi_l$ or $\phi_i = \phi_l$, $\phi_j = \phi_k$ in equation (8) [4]. It has also been assumed that there is no correlation between the low-order scattering part and the diffusive-scattering part.

As we mentioned before, the absorption of the medium does not change the statistical properties of the diffusive-scattering part, except for a decrease in the average intensity $\langle I_m \rangle \equiv \sum_{i=j}^{N} \langle |A_i|^2 \rangle$, which obeys Rayleigh statistics. Therefore, what we should discuss is a variation in the average intensity $\langle I_c \rangle \equiv \langle |A_c|^2 \rangle$ of the low-order scattering part and the second-order moment $\langle I_c^2 \rangle \equiv \langle |A_c|^4 \rangle$ in equations (7) and (8). As a rough approximation, we assume that the low-order scattering part is constituted only by a single-scattering component. The probability density function of path length distributions for the single-scattering component is represented by

$$p(s_c) = \frac{1}{2l} \exp\left(-\frac{s_c}{2l}\right) \tag{9}$$

where s_c and l denote the path length of the single-scattered wave and the mean free path of the scattering medium, respectively. Equation (9) means that a random variable s_c denotes the

distance of an optical path which is folded by the first scattering event. The average intensity of the low-order scattering part is then given by

$$\begin{aligned}\langle I_c \rangle &= \int_0^\infty \overline{I_c} \exp\left(-\frac{s_c}{l_a}\right) p(s_c)\, \mathrm{d}s_c \\ &= \frac{\overline{I_c}}{1+2\gamma}\end{aligned} \tag{10}$$

where $\overline{I_c}$ denotes the intensity of the single-scattering component for non-absorbing media. The factor γ is again the normalized absorption coefficient of $\gamma = (l_a/l)^{-1}$. The second-order moment is also derived as

$$\begin{aligned}\langle I_c^2 \rangle &= \int_0^\infty \overline{I_c}^2 \exp\left(-\frac{2s_c}{l_a}\right) p(s_c)\, \mathrm{d}s_c \\ &= \frac{(1+2\gamma)^2}{1+4\gamma}\langle I_c \rangle^2.\end{aligned} \tag{11}$$

Therefore, equation (8) is rewritten as

$$\langle I^2 \rangle = \frac{(1+2\gamma)^2}{1+4\gamma}\langle I_c \rangle^2 + 4\langle I_c \rangle\langle I_m \rangle + 2\langle I_m \rangle^2. \tag{12}$$

Finally, the speckle contrast is represented by

$$\begin{aligned}C &= \frac{\sqrt{\langle I^2 \rangle - \langle I \rangle^2}}{\langle I \rangle} \\ &= \left(\frac{[(1+2\gamma)^2/(1+4\gamma) - 1]R_a^2 + 2R_a + 1}{R_a^2 + 2R_a + 1}\right)^{1/2}\end{aligned} \tag{13}$$

where $R_a \equiv \langle I_c \rangle / \langle I_m \rangle$ is the average intensity ratio of the low-order scattering (single-scattering) part to the diffusive-scattering part, and varies depending on the sample thickness, the scattering anisotropy, and also the factor γ.

In figure 6 we plot a variation of the contrast given in equation (13) against γ and R_a. The contrast is almost independent of the absorption coefficient for small R_a because multiple scattering is dominant in this regime. On the other hand, it varies dramatically for large R_a in which the single-scattering component is dominant. As we mentioned above, the ratio R_a also varies depending on such factors as the sample thickness, the scattering anisotropy and the absorption coefficient. In particular, the value of R_a increases with an increase of γ owing to the depletion of multiple-scattering waves. Therefore, a dip in the contrast which appears in the weak absorption regime in figures 3 and 4 is readily reproduced by tracing the plot in figure 6 diagonally.

Using equation (13), we evaluate the ratio R_a from a particular value of γ and the contrast value at the point obtained by numerical simulations shown in figures 3 and 4. Figure 7 shows the ratio R_a as a function of the absorption coefficient with the value of the parameters being the same as in figures 3 and 4. We can also obtain directly from simulation data the ratio R_{sm} of the averaged single-scattering intensity to the averaged multiple-scattering intensity which includes more than the second-order scattering components. The results are shown in figure 8, indicating that the multiple-scattering components become less significant than the single-scattering component with an increase of the absorption. An increase of the ratio R_a is also observed for the weak absorption ($\gamma < 0.1$) in figure 7. The value of R_a is larger than that of R_{sm} in this region, since the low-order multiple-scattering components, which have been ignored in this theoretical model, also cause a decrease in the speckle contrast for non-absorbing media.

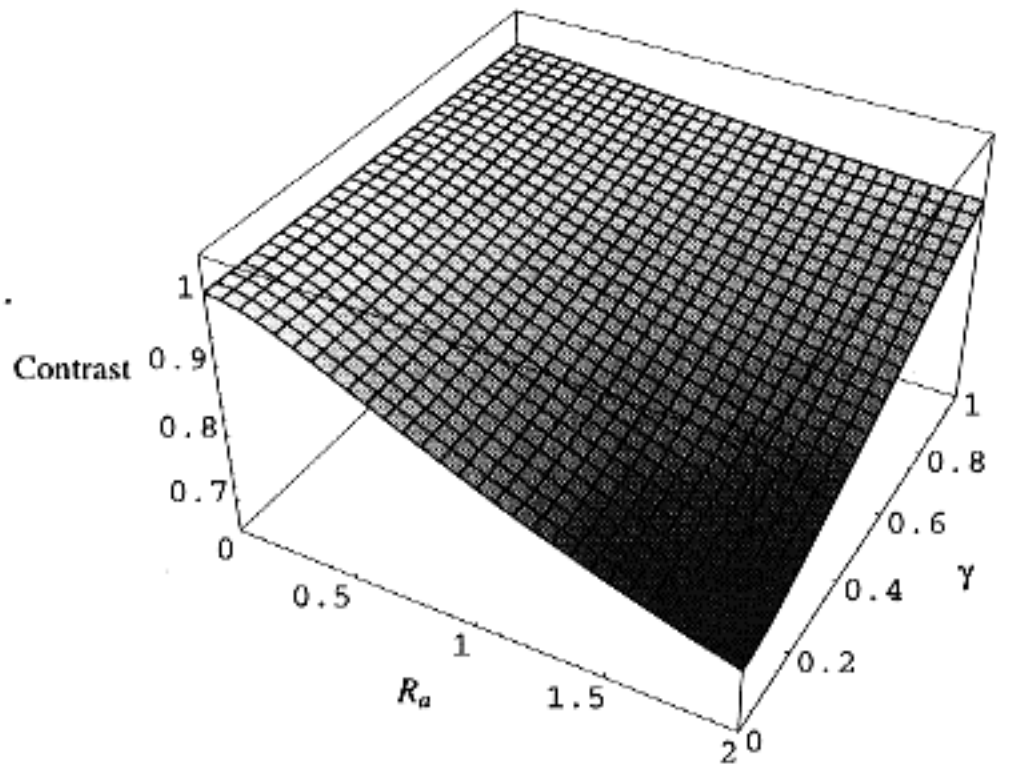

Figure 6. Speckle contrast versus the absorption coefficient γ and the ratio of the low-order scattering components to the diffusive-scattering components R_a, based on the single-scattering approximation.

On the other hand, the value of R_a decreases in the strong absorption regime in figure 7. This is inconsistent with the fact shown in figure 8 that the absorption depletes the multiple-scattering components. This change of the ratio R_a is also caused by the contribution of the low-order multiple-scattering components. The longer optical path induces a larger amplitude modulation due to absorption for the low-order multiple-scattering components than for the single-scattering component. In this case, the low-order multiple-scattering components behave like the diffusive-scattering part in our theoretical model, and suppress the ratio R_a in

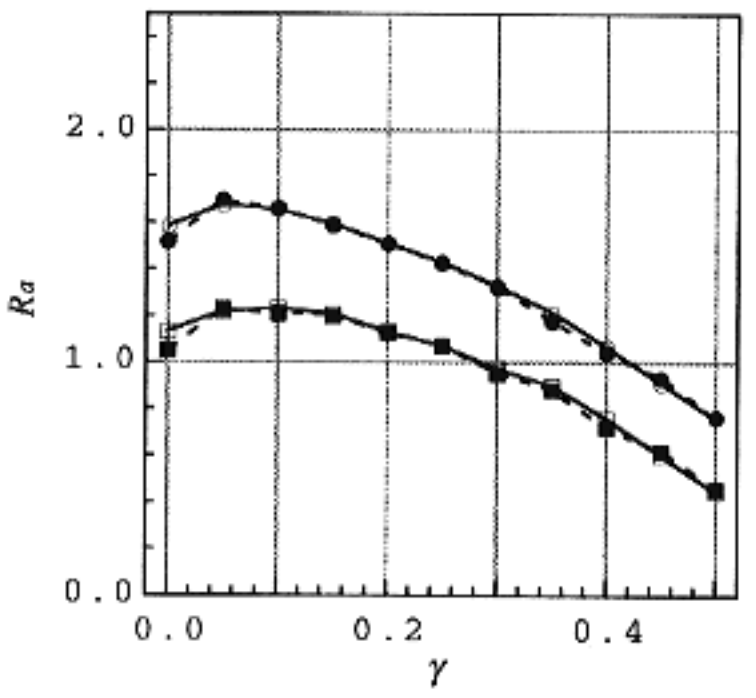

Figure 7. Average intensity ratio R_a of the low-order scattering components to the diffusive-scattering components with the asymmetry factors of $g = 0$ (circles) and 0.33 (squares). The symbols ○ and □ represent the data for the sample thickness $L = 5$, and the symbols ● and ■ for $L = 15$.

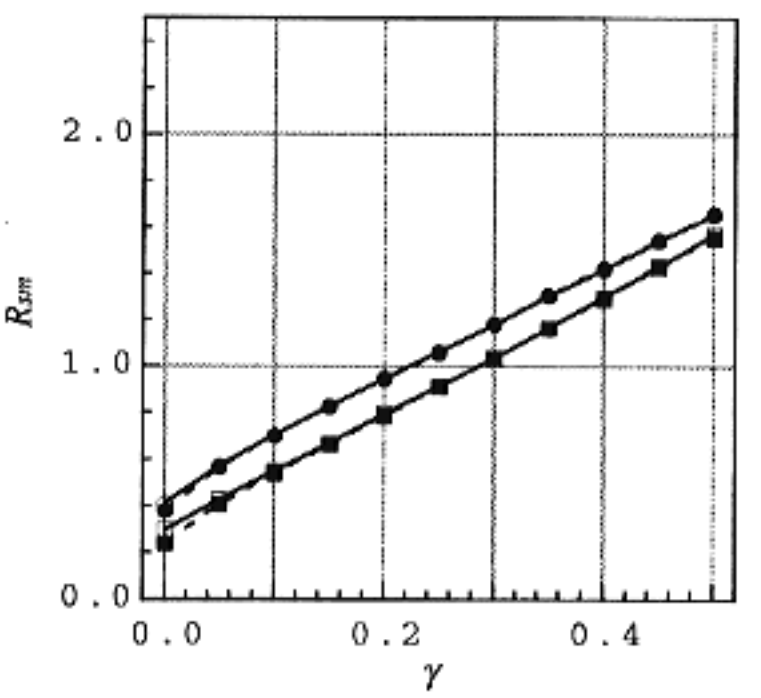

Figure 8. Average intensity ratio R_{sm} of the single-scattering intensity to the multiple-scattering intensity with asymmetry factors of $g = 0$ (circles) and 0.33 (squares). The symbols ○ and □ represent the data for the sample thickness $L = 5$, and the symbols ● and ■ for $L = 15$.

the strong absorption regime. On the other hand, the discrepancy of the ratios R_a for $g = 0$ and 0.33 in figure 7 is caused not only by the difference between the intensity ratios of the single-scattering component to the multiple-scattering components, but also by the contribution of the low-order multiple-scattering components which are more dominant in the strong scattering case of $g = 0$ than in the weak scattering case of $g = 0.33$. The latter contribution is shown in figure 7 where the curve of R_a decreases faster for $g = 0$ than for $g = 0.33$ with an increase of the absorption coefficient.

5. Conclusion

We have discussed a variation in the contrast of speckle patterns which are formed by the backscattered light at the surface of random media. It was shown from numerical simulations that the contrast first decreases in the weak absorption regime and then gradually increases with an increase of the absorption coefficient. In order to elucidate the reasons for such a contrast variation to occur, we proposed a simple theoretical model in which the scattered light consists of two different components of the low-order scattering and the diffusive scattering contributing differently to the speckle patterns. The theoretical approach explains qualitatively a change in the speckle contrast. However, our estimation obtained with the single-scattering approximation for the low-order scattering components deviates from the results of numerical simulations. This reflects the contribution of the second- and higher-order scattering waves which are ignored in our theoretical model, and they have more effect on the properties of backscattered light in the strong scattering regime of $g = 0$ than in the weak scattering regime of $g = 0.33$.

For real experiments, the contributions of the single scattering and the low-order scattering are smaller than those in our simulations, because we have restricted the scattering direction only to the orthogonal directions. However, if we go beyond the strong scattering regime, we will eventually reach a wave localized state, and the number of optical paths which can exist in random scattering media is restricted to a smaller number than in the weak scattering regime. In this situation, the contrast variation depending on the strength of the absorption may be observed in the backscattered light.

References

[1] Stephen M J and Cwilich G 1987 Intensity correlation functions and fluctuations in light scattered from a random medium *Phys. Rev. Lett.* **59** 285–7

[2] Feng S, Kane C, Lee P A and Stone A D 1988 Correlation and fluctuations of coherent wave transmission through disordered media *Phys. Rev. Lett.* **61** 834–7

[3] de Boer J F, van Albada M P and Lagendijk A 1992 Transmission and intensity correlations in wave propagation through random media *Phys. Rev.* B **45** 658–66

[4] Shnerb N and Kaveh M 1991 Non-Rayleigh statistics of waves in random systems *Phys. Rev.* B **43** 1279–82

[5] Kogan E, Kaveh M, Baumgartner R and Berkovits R 1993 Statistics of waves propagating in a random medium *Phys. Rev.* B **48** 9404–10

[6] Genack A Z and Garcia N 1993 Intensity statistics and correlation in absorbing media *Europhys. Lett.* **21** 753–8

[7] Nieuwenhuizen Th M and van Rossum M C W 1995 Intensity distributions of waves transmitted through a multiple scattering medium *Phys. Rev. Lett.* **74** 2674–7

[8] Akkermans E, Wolf P E and Maynard R 1986 Coherent backscattering of light by disordered media: analysis of the peak line shape *Phys. Rev. Lett.* **56** 1471–4

[9] Wolf P E, Maret G, Akkermans E and Maynard R 1988 Optical coherent backscattering by random media: an experimental study *J. Physique* **49** 63–75

[10] Wiersma D S, van Albada M P, van Tiggelen B A and Lagendijk A 1995 Experimental evidence for recurrent multiple scattering events of light in disordered media *Phys. Rev. Lett.* **74** 4193–6

[11] Pnini R and Shapiro B 1991 Intensity correlation in absorbing random media *Phys. Lett.* A **157** 265–9

[12] Kogan E and Kaveh M 1992 Effect of absorption on long-range correlations in random media *Phys. Rev.* B **45** 1049–51

[13] Edrei I, Kaveh M and Shapiro B 1989 Probability distribution functions for transmission of waves through random media: a new numerical method *Phys. Rev. Lett.* **62** 2120–3

[14] Berkovits R and Feng S 1994 Correlation in coherent multiple scattering *Phys. Rep.* **238** 135–72

[15] Sangu S, Okamoto T and Asakura T 1998 Anomalous correlation of intensity fluctuations in strong scattering media *J. Mod. Opt.* **45** 117–32

[16] Soto-Crespo J M and Nieto-Vesperinas M 1989 Electromagnetic scattering from very rough surfaces and deep reflection gratings *J. Opt. Soc. Am.* A **6** 367–84